

This is an Open Access document downloaded from ORCA, Cardiff University's institutional repository: <https://orca.cardiff.ac.uk/id/eprint/144446/>

This is the author's version of a work that was submitted to / accepted for publication.

Citation for final published version:

Mashruk, Syed, Kovaleva, Marina , Zitouni, Seif Eddine, Brequigny, Pierre, Rousselle, Christine and Valera-Medina, Agustin 2021. Ammonia/hydrogen/methane characteristic profiles for atmospheric combustion applications. Presented at: 13th International Conference on Applied Energy (ICAE 2021), Bangkok, Thailand, 29 November - 02 December 2021. Energy Proceedings. 10.46855/energy-proceedings-9188

Publishers page: <https://doi.org/10.46855/energy-proceedings-9188>

Please note:

Changes made as a result of publishing processes such as copy-editing, formatting and page numbers may not be reflected in this version. For the definitive version of this publication, please refer to the published source. You are advised to consult the publisher's version if you wish to cite this paper.

This version is being made available in accordance with publisher policies. See <http://orca.cf.ac.uk/policies.html> for usage policies. Copyright and moral rights for publications made available in ORCA are retained by the copyright holders.



# Ammonia/Hydrogen/Methane Characteristic Profiles for Atmospheric Combustion Applications

Mashruk S<sup>1</sup>, Kovaleva M<sup>1</sup>, Zitouni SE<sup>2</sup>, Brequigny P<sup>2</sup>, Mounaim-Rouselle C<sup>2</sup>, Valera-Medina A<sup>1</sup>

<sup>1</sup>College of Physical Sciences and Engineering, Cardiff University, UK

<sup>2</sup>PRISMA, University of Orleans, Orleans, France

## ABSTRACT

Ammonia has become a chemical of interest for the economic distribution and storage of hydrogen. Utilization of this molecule has been conceived in systems that range from small Fuel Cells to large gas turbines and furnaces. Ammonia characteristics enable the reduction of carbon emissions whilst ensuring long term storage and distribution of hydrogen produced from renewable sources. However, the use of ammonia as a combustion fuel also presents various issues mainly related to low flame speed and elevated nitrogen-based emissions. Therefore, further understanding of this molecule and its combustion characteristics is required before replacement of fossil fuels using ammonia can be accomplished at large scale. Therefore, this work presents a series of experiments that depict the characteristic profiles of various ammonia/hydrogen/methane blends intended to serve as replacement of pure fossil-based fuelling sources. The study is approached through a generic tangential swirl burner which has been commissioned to burn a great variety of blends at various power outputs. Temperatures, operability, chemiluminescence of various species ( $\text{OH}^*$ ,  $\text{NH}_2^*$ ,  $\text{CH}^*$  and  $\text{NH}^*$ ), spectrometry profiles, and emissions were determined for comparison purposes at various equivalence ratios and blending conditions.

**Keywords:** Ammonia, hydrogen, combustion, power generation.

## 1. INTRODUCTION

Ammonia combustion has recently received considerable attention, not only because ammonia can be used as a cheap method to distribute hydrogen over long distances and enable storage for long periods of time, but also because ammonia presents a unique opportunity to achieve low emissions power generation. Recent analyses [1]

suggest that the use of ammonia/hydrogen combustion might lead to  $\text{NO}_x$  emissions below 10 ppm, whilst other works [2–4] acknowledge the use of ammonia blends for medium, reliable power sourced by stranded or green renewable sources. The works have led to the search of blends and conditions that range from lean high hydrogen content  $>30\%$  (vol) [5,6] to multi-stage combustion concepts [7,8], from small scale burners [9] to large power generation [10,11]. Furthermore, new models, combustion rigs and reaction mechanisms have been conceived to determine the feasibility of using not only hydrogen, but also other molecules such as methane, propane, octane, various syngases, etc. thus increasing the versatility of ammonia for combustion purposes [12–17].

However, there are still many unknowns on how these various blends can impact over the production of emissions such as  $\text{N}_2\text{O}$ ,  $\text{NO}_2$ , unburned ammonia and CO. Many of these blends, which will be initially employed for the transition to pure hydrogen systems might not provide feasible outputs under current legislations, whilst others might pose a challenge for operability and flame stability. Therefore, this manuscript is intended to provide further recognition to various ammonia/hydrogen/methane blends in order to derive useful information for modellers and potential users, thus showing a comparison between different conditions of operation whilst addressing the production of emissions and temperature profiles. The study is complemented with spectrometric analyses and chemiluminescence imagery of species such as  $\text{OH}^*$ ,  $\text{NH}^*$ ,  $\text{NH}_2^*$  and  $\text{CH}^*$ , all radicals that are well known to contribute to the production of molecules such as CO,  $\text{CO}_2$ ,  $\text{NO}_x$ ,  $\text{N}_2$  and water.

## 2. METHODOLOGY

A tangential swirl burner was employed at 8kW power and 1.04 swirl, Figure 1. The unit was fed using Bronkhorst massflow controllers that enabled a precision of 0.5% within a range of 15-95% massflow. The unit was fed using hydrogen, ammonia and methane as in table 2. CH<sub>4</sub> and NH<sub>3</sub> was fully premixed with air, while H<sub>2</sub> was introduced 4 cm below the burner exit into the swirl to ensure premixing. Various conditions were assessed to determine the impact of equivalence ratio on temperature, emissions, spectroscopy and radical formation.

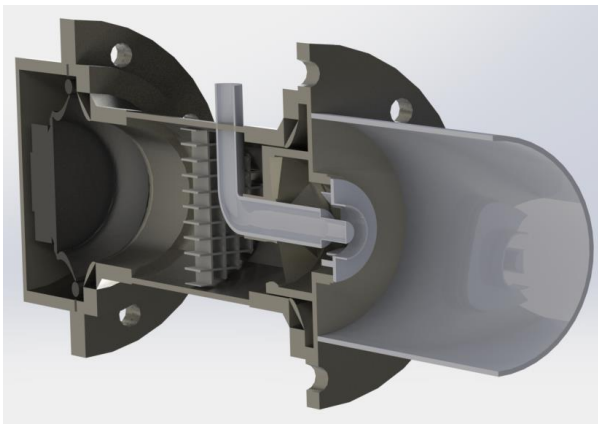


Fig. 1. Tangential combustor.

Table 2. Experimental matrix.

TP	CH <sub>4</sub> (vol.%)	NH <sub>3</sub> (vol.%)	H <sub>2</sub> (vol.%)	Equivalence Ratio ( $\Phi$ )
1	0	90	10	0.8
2	0	90	10	1.0
3	0	90	10	1.2
4	0	100	0	0.8
5	0	100	0	1.0
6	0	100	0	1.2
7	100	0	0	0.8
8	100	0	0	1.0
9	100	0	0	1.2
10	30	0	70	0.8
11	30	0	70	1.0
12	30	0	70	1.2
13	20	80	0	0.8
14	20	80	0	1.0
15	20	80	0	1.2
16	40	60	0	0.8
17	40	60	0	1.0
18	40	60	0	1.2
19	60	40	0	0.8

20	60	40	0	1.0
21	60	40	0	1.2

Experiments were conducted at atmospheric pressure and inlet temperature. A pair of LaVision CCD cameras were employed to obtain chemiluminescence traces of various species. The units were triggered simultaneously with a gate timing of 700000 ns and a gain of 90%. Various Edmond filters were used for each species namely OH\* (310 nm), CH\* (420 nm), NH\* (337 nm) and NH<sub>2</sub>\* (632 nm). LaVision Davis v10 was used to gather 200 instantaneous images per species, which were then post-processed using a bespoke Matlab script designed to conduct Abel Deconvolution averaging. Temperature profiles were obtained via K and R type thermocouples plugged into an RS data logger directly linked to a computer. The thermocouples were previously calibrated showing an average error of 3%. Emissions (NO, N<sub>2</sub>O, NO<sub>2</sub>, NH<sub>3</sub>, CO, CO<sub>2</sub>, O<sub>2</sub> and H<sub>2</sub>O) were all measured using a bespoke Emerson CT5100 Quantum Cascade Laser analyser at a frequency of 1 Hz, a repeatability of  $\pm 1\%$ , 0.999 linearity, and sampling temperature up to 190°C. A heated line at 160°C was employed to avoid condensation. Finally, a Blue-Wave StellarNet CMOS spectrometer with a detector ranging from 200 to 1100 nm was focused on the flame core. 20 data points were averaged for better resolution. An embedded software (SpectraWiz) was used to record the spectrographic signatures of all flames.

## 3. RESULTS

Chemiluminescence data, Fig. 2, showed some expected trends in the blends used. For example, the presence of CH\* was an expected characteristic of high methane content flames that was not observed in the carbon-free blends. However, there were other trends that denoted unexpected behaviour of each blend. NH\* was observed in high concentration when pure methane was used, a trend that decayed into higher NH<sub>2</sub>\* patterns at higher equivalence ratios. As it has been demonstrated by others [18,19], it is the presence of NH<sub>2</sub> that can enable reduction of NO emissions, although the presence of M+ species can also trigger the conversion towards HNO, parameters that need to be linked to other conditions.

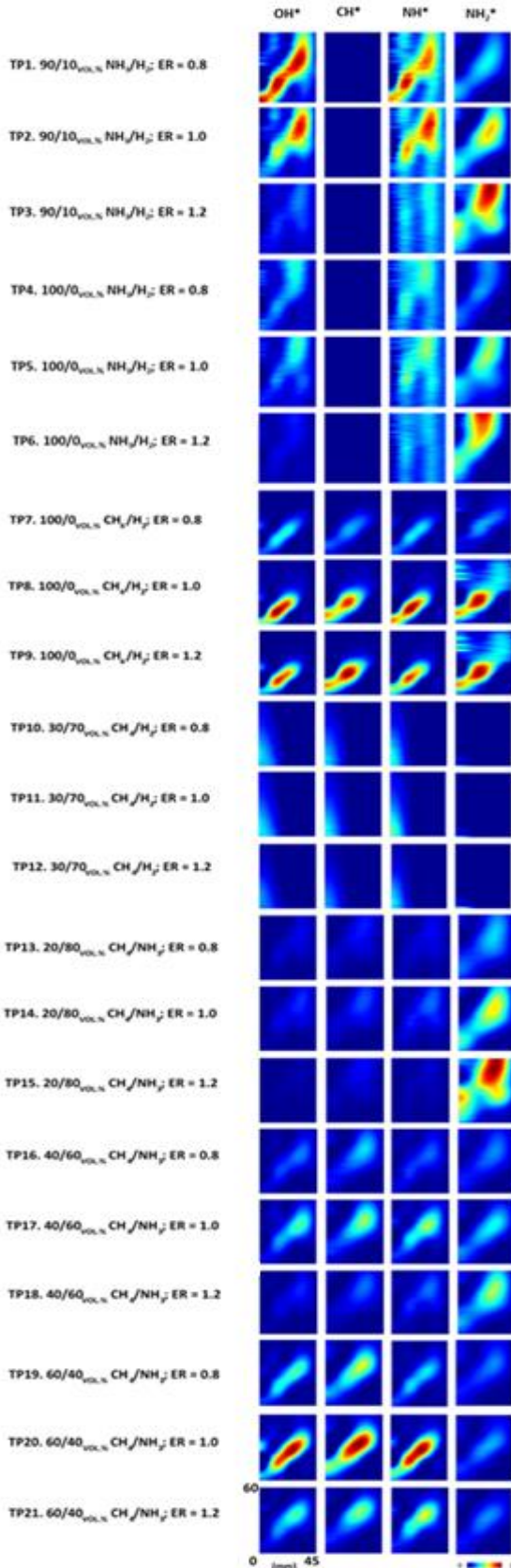


**Fig. 2.** Chemiluminescence results for OH\*, CH\*, NH\* and NH<sub>2</sub>\*. Colourmap normalised to image dataset (TP 1-6; 7-12; 13-21) max.

Further, it is clear that the presence of ammonia traces at low equivalence ratios tends to form OH radicals, whilst higher equivalence ratios led to higher NH<sub>2</sub> formation. The trend is also evident at pure ammonia concentrations, thus affirming that OH\* has a less prone contribution at high equivalence ratios. The behaviour is linked to the reduced oxygen content at high equivalence ratios. This is also a contributor to the reduction of emissions via the formation of NH → HNO, since the formation of NH via the reaction NH<sub>2</sub> + OH → NH + H<sub>2</sub>O is highly sensitive under lean conditions [20]. Similarly, high hydrogen content only denoted formation of NH\* with minor traces of NH<sub>2</sub>\* when ammonia was not used, thus eliminating the contributing support for NO<sub>x</sub> reduction via NH<sub>2</sub> + NO → N<sub>2</sub> + H<sub>2</sub>O. Interestingly, high amidogen (NH<sub>2</sub>) trends were observed with low CH\* formation at low methane content (20/80 CH<sub>4</sub>/NH<sub>3</sub>), whilst a considerably weaker performance of amidogen and higher CH\* were produced at higher methane concentrations.

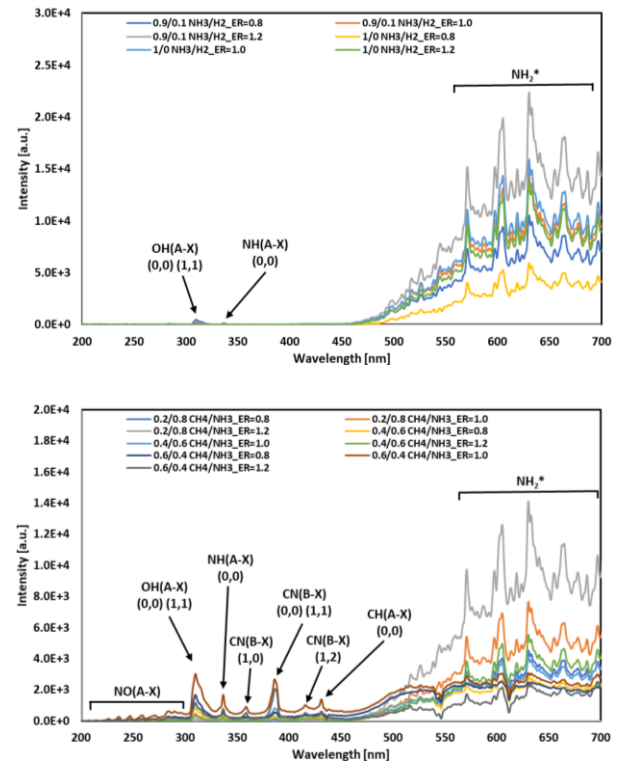


**Fig. 3.** Spectrometry results. Top) Cases 1-6, Table 2. Bottom) Cases 13-21.

However, there is evidence that NH<sub>2</sub>\* was produced at its highest value under all rich



conditions, Fig 3. This can potentially be also a product of the recombination of  $\text{NH}$  at lower temperatures, thus leading to the formation of  $\text{NH}_2$  and  $\text{NNH}$ , both known species to have high sensitivity to  $\text{NO}$  production/destruction. It was also found that  $\text{CN}$ ,  $\text{CH}$  and  $\text{NO}$  signatures were at the highest value under stoichiometric conditions when methane was used at high concentration (60%). These radicals are known to preclude  $\text{CO}$  and soot formation, whilst  $\text{NO}$  can finish recombining into  $\text{NO}_2$  and/or  $\text{N}_2\text{O}$ . This, in comparison, was not the case at 1.2 equivalence ratios, which shows one of the weakest signals for these species.

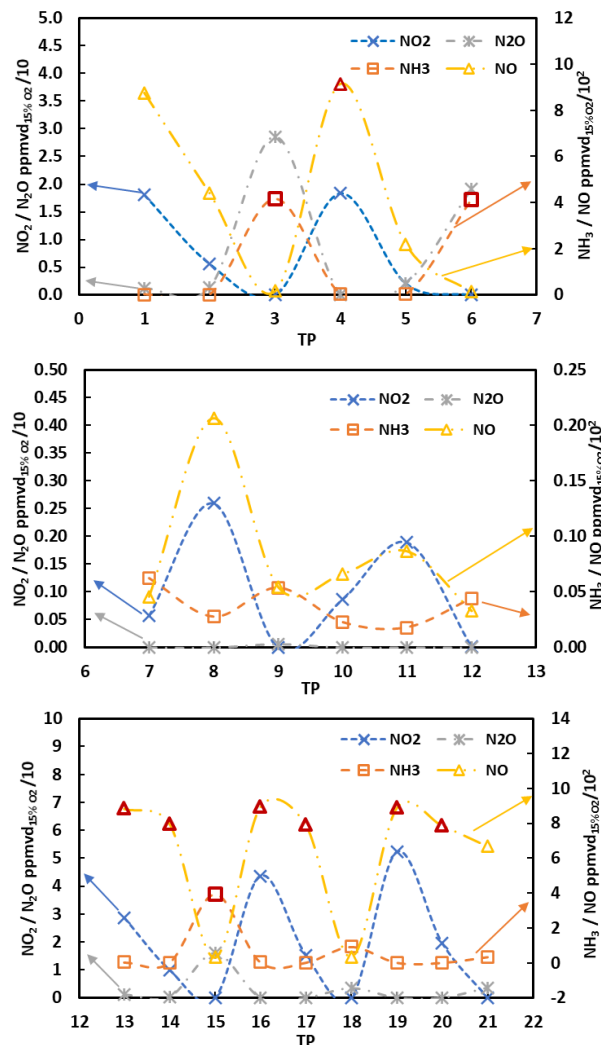


**Fig. 4.**  $\text{NO}_2$ ,  $\text{N}_2\text{O}$ ,  $\text{NH}_3$  and  $\text{NO}$  emissions. Top) Cases 1-6; Middle) Cases 7-12; Bottom) Cases 13-21. Red markers indicate greater than values.

In terms of exhaust emissions (Fig. 4) and temperature, an interesting pattern was observed

between cases. Those that did not have methane presented the highest temperatures at the outlet (with an average of  $\sim 1235$  K), whilst those with methane showed considerably lower temperature profiles (with an average of  $\sim 1197$  K). This result leads to the recognition of longer flames and post-combustion processes that do not occur when methane is present, potentially a consequence of shorter flames. Herein, it would be expected that the longer presence of ammonia would affect emission profiles. With no carbon content, no  $\text{CO}/\text{CO}_2$  was observed for the first cases. Also, the higher ammonia content and longer flames enable recombination of species, considerably limiting the production of  $\text{NO}$ . Interestingly, rich conditions also lead to higher  $\text{N}_2\text{O}$  production, a trend that is opposite to  $\text{NO}_2$  which shows its highest values under lean conditions. The effect changes without ammonia, as expected, with stoichiometric conditions showing the dirtiest patterns in terms of  $\text{NO}_x$  production. Finally, ammonia and methane flames show the poorest performance in the production of  $\text{NO}$ . However, ammonia profiles are relatively good with concentrations in the tenths, whilst  $\text{N}_2\text{O}$  shows values below single digits under most combinations. As expected,  $\text{NO}_2$  peaks under lean conditions. These results are extremely encouraging in defining clean-up strategies for these combustion cases. High ammonia-zero carbon blends might require tackling  $\text{N}_2\text{O}$  with unburned ammonia, whilst methane-ammonia blends can benefit from  $\text{NO}$  abatement techniques at the flame core.

#### 4. CONCLUSIONS

Series of tests were conducted to determine ammonia combustion features at various equivalence ratios. It was found that  $\text{NH}_2^*$ , a radical with high deNO<sub>x</sub> potential, is mainly formed at rich conditions in most combinations. Although the presence of ammonia produces low  $\text{NO}$  at high equivalence ratios, concerns might be posed on  $\text{N}_2\text{O}$ . Simultaneously, methane blends can be concerning around  $\text{NO}$  production, thus requiring different abatement techniques for cleaner power production.

## Acknowledgements

The authors gratefully acknowledge the support from European Union's H2020 program through the project Flex&Confu (no. 884157).

## References

- [1] Pugh D, Valera-Medina A, Bowen P, Giles A, Goktepe B, Runyon J, et al. Emissions Performance of Staged Premixed and Diffusion Combustor Concepts for an NH<sub>3</sub>/Air Flame With and Without Reactant Humidification. *J Eng Gas Turbines Power* 2020;1–10. <https://doi.org/10.1115/1.4049451>.
- [2] Colson S, Hirano Y, Hayakawa A, Kudo T, Kobayashi H, Galizzi C, et al. Experimental and Numerical Study of NH<sub>3</sub>/CH<sub>4</sub> Counterflow Premixed and Non-premixed Flames for Various NH<sub>3</sub> Mixing Ratios. *Combust Sci Technol* 2020. <https://doi.org/10.1080/00102202.2020.1763326>.
- [3] Okafor EC, Yamashita H, Hayakawa A, Somarathne KDKA, Kudo T, Tsujimura T, et al. Flame stability and emissions characteristics of liquid ammonia spray co-fired with methane in a single stage swirl combustor. *Fuel* 2020;287:119433. <https://doi.org/10.1016/j.fuel.2020.119433>.
- [4] Mounaïm-Rousselle C, Brequigny P. Ammonia as Fuel for Low-Carbon Spark-Ignition Engines of Tomorrow's Passenger Cars. *Front Mech Eng* 2020;6:70.
- [5] Valera-Medina A, Pugh DG, Marsh P, Bulat G, Bowen P. Preliminary study on lean premixed combustion of ammonia-hydrogen for swirling gas turbine combustors. *Int J Hydrogen Energy* 2017. <https://doi.org/10.1016/j.ijhydene.2017.08.028>.
- [6] Khateeb AA, Guiberti TF, Zhu X, Younes M, Jamal A, Roberts WL. Stability limits and NO emissions of technically-premixed ammonia-hydrogen-nitrogen-air swirl flames. *Int J Hydrogen Energy* 2020;45:22008–18. <https://doi.org/10.1016/j.ijhydene.2020.05.236>.
- [7] Pugh D, Bowen P, Valera-Medina A, Giles A, Runyon J, Marsh R. Influence of steam addition and elevated ambient conditions on NO<sub>x</sub> reduction in a staged premixed swirling NH<sub>3</sub>/H<sub>2</sub> flame. *Proc Combust Inst* 2019;37:5401–9. <https://doi.org/10.1016/j.proci.2018.07.091>.
- [8] Okafor EC, Somarathne KDKA, Ratthan R, Hayakawa A, Kudo T, Kurata O, et al. Control of NO<sub>x</sub> and other emissions in micro gas turbine combustors fuelled with mixtures of methane and ammonia. *Combust Flame* 2020;211:406–16. <https://doi.org/10.1016/j.combustflame.2019.10.012>.
- [9] Franco MC, Rocha RC, Costa M, Yehia M. Characteristics of NH<sub>3</sub>/H<sub>2</sub>/air flames in a combustor fired by a swirl and bluff-body stabilized burner. *Proc Combust Inst* 2020;38. <https://doi.org/10.1016/j.proci.2020.06.141>.
- [10] Guteša Božo, M. Mashruk, S. Zitouni, S. Valera-Medina A. Humidified Ammonia/Hydrogen RQL combustion in a Trigeneration Gas Turbine Cycle. *Energy Convers Manag* 2020.
- [11] Ito S, Uchida M, Onishi S, Fujimori T, Kobayashi T. Performance of Ammonia–Natural Gas Co-fired Gas Turbine for Power Generation. *NH<sub>3</sub> Assoc* 2018. <https://nh3fuelassociation.org/wp-content/uploads/2018/12/1545-Performance-of-Ammonia–Natural-Gas-for-Power-Generation-for-Power-Generation.pdf> (accessed June 24, 2019).
- [12] Xiao H, Lai S, Valera-Medina A, Li J, Liu J, Fu H. Experimental and modeling study on ignition delay of ammonia/methane fuels. *Int J Energy Res* 2020;44:6939–49. <https://doi.org/10.1002/er.5460>.
- [13] Lubrano Lavadera M, Han X, A. Konnov A. Comparative Effect of Ammonia Addition on the Laminar Burning Velocities of Methane, n-Heptane, and Iso-octane. *Energy & Fuels* 2020;0. <https://doi.org/10.1021/acs.energyfuels.0c03424>.
- [14] Mei B, Ma S, Zhang Y, Zhang X, Li W, Li Y. Exploration on laminar flame propagation of ammonia and syngas mixtures up to 10 atm. *Combust Flame* 2020;220:368–77. <https://doi.org/10.1016/j.combustflame.2020.07.011>.
- [15] Chen J, Jiang X, Qin X, Huang Z. Effect of hydrogen blending on the high temperature auto-ignition of ammonia at elevated pressure. *Fuel* 2021;287:119563. <https://doi.org/10.1016/j.fuel.2020.119563>.
- [16] Valera-Medina A, Amer-Hatem F, K. Azad A, C. Dedoussi I, de Joannon M, X. Fernandes R, et al. Review on Ammonia as a Potential Fuel: From Synthesis to Economics. *Energy & Fuels* 2021;0. <https://doi.org/10.1021/acs.energyfuels.0c03685>.
- [17] Mikulčić H, Baleta J, Wang X, Wang J, Qi F, Wang F. Numerical simulation of ammonia/methane/air combustion using reduced chemical kinetics models. *Int J Hydrogen Energy* 2021. <https://doi.org/10.1016/j.ijhydene.2021.01.109>.
- [18] Glarborg P, Miller JA, Ruscic B, Klippenstein SJ. Modeling nitrogen chemistry in combustion. *Prog Energy Combust Sci* 2018;67:31–68. <https://doi.org/10.1016/j.peccs.2018.01.002>.
- [19] Valera-Medina A, Mashruk S, Xiao H, Chiong M-C, Tung Chong C. Ammonia/Hydrogen Blends for Zero-Carbon Energy. 2020.
- [20] Mashruk, S. Xiao, H. Valera-Medina A. Rich-Quench-Lean model comparison for the clean use of humidified ammonia/hydrogen combustion systems. *Int J Hydrogen Energy* 2020.